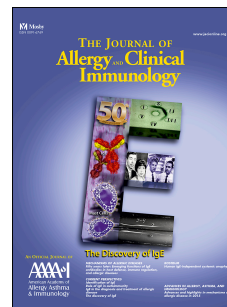# Accepted Manuscript

Persistent kallikrein5 activation induces atopic dermatitis-like skin architecture independent of PAR2 activity

Yanan Zhu, PhD, Joanne Underwood, PhD, Derek Macmillan, PhD, Leila Shariff, PhD, Ryan O'Shaughnessy, PhD, John I. Harper, MD FRCP FRCPCH, Chris Pickard, PhD, Peter S. Friedmann, MD FRCP FMedSci, Eugene Healy, MB PhD FRCP FRSB, Wei-Li Di, MBBS PhD

Please cite this article as: Zhu Y, Underwood J, Macmillan D, Shariff L, O'Shaughnessy R, Harper JI, Pickard C, Friedmann PS, Healy E, Di W-L, Persistent kallikrein5 activation induces atopic dermatitis-like skin architecture independent of PAR2 activity, *Journal of Allergy and Clinical Immunology* (2017), doi: 10.1016/j.jaci.2017.01.025.

This is a PDF file of an unedited manuscript that has been accepted for publication. As a service to our customers we are providing this early version of the manuscript. The manuscript will undergo copyediting, typesetting, and review of the resulting proof before it is published in its final form. Please note that during the production process errors may be discovered which could affect the content, and all legal disclaimers that apply to the journal pertain.

1   **Persistent kallikrein5 activation induces atopic dermatitis-like skin**

2   **architecture independent of PAR2 activity**

3   Yanan Zhu[1] PhD, Joanne Underwood[2] PhD, Derek Macmillan[3] PhD, Leila Shariff[3] PhD, Ryan

4   O'Shaughnessy[1] PhD, John I. Harper[1] MD FRCP FRCPCH, Chris Pickard[2] PhD, Peter S.

5   Friedmann[2] MD FRCP FMedSci, Eugene Healy[2,4] MB PhD FRCP FRSB , Wei-Li Di[1] MBBS PhD

6

7   1. Infection, Immunity, Inflammation and Physiological Medicine Programme, Immunobiology

8   Section, UCL Institute of Child Health, 30 Guildford Street, London WC1N 1EH, UK.

9   2. Dermatopharmacology, Sir Henry Wellcome Laboratories, Faculty of Medicine, University of

10   Southampton, Southampton General Hospital, SO16 6YD, UK

11   3. Department of Chemistry, University College London, 20 Gordon Street, WC1H 0AJ, UK.

12   4. Dermatology, University Hospital Southampton NHS Foundation Trust, Southampton, SO16

13   6YD, UK

14   **Corresponding Author**:

15   Dr. Wei-Li Di, MBBS, PhD

16   Senior Lecturer,

17   UCL Institute of Child Health, Immunobiology Section,

18   30 Guildford Street, London WC1N 1EH, UK.

19   Tel: 44 (0)20 79052369

20   Fax: 44 (0)20 78138494

21   E-mail w.di@ucl.ac.uk

22   **Conflicts of interest**:

23   none

Abstract

Background: Up-regulation of kallikreins (KLK) including KLK5 has been reported in atopic dermatitis (AD). KLK5 has biological functions which include degrading desmosomal proteins and inducing pro-inflammatory cytokine secretion through protease activated receptor 2 (PAR2). However, due to the complex interactions between various cells in AD inflamed skin, it is difficult to dissect the precise and multiple roles of up-regulated KLK5 in AD skin.

Objective: We investigated the effect of up-regulated KLK5 on the expression of epidermal related proteins and cytokines in keratinocytes and on skin architecture.

Methods: Lesional and non-lesional AD skin biopsies were collected for analysis of morphology and protein expression. The relationship between KLK5 and barrier related molecules was investigated using an *ex-vivo* dermatitis skin model with transient KLK5 expression and a cell model with persistent KLK5 expression. The influence of up-regulated KLK5 on epidermal morphology was investigated using an *in vivo* skin graft model.

Results: Up-regulation of KLK5 and abnormal expression of desmoglein 1 (DSG1) and filaggrin (FLG), but not PAR2 were identified in AD skin. PAR2 was increased in response to transient up-regulation of KLK5, while persistently up-regulated KLK5 did not show this effect. Persistently up-regulated KLK5 degraded DSG1 and stimulated secretion of IL-8, IL-10 and TSLP independent of PAR2 activity. With control of higher KLK5 activity by the inhibitor SFTI-G, restoration of DSG1 expression and a reduction in AD-related cytokine IL-8, TLSP and IL-10 secretion were observed. Furthermore, persistently elevated KLK5 could induce AD-like skin architecture in an *in vivo* skin graft model. .

Conclusion: Persistently up-regulated KLK5 resulted in AD-like skin architecture and secretion of AD-related cytokines from keratinocytes in a PAR-2 independent manner. Inhibition of KLK5-mediated effects may offer potential as a therapeutic approach in AD.

Key messages

- Persistently up-regulated KLK5 induces PAR2-independent IL-8, IL10 and TSLP secretion, causing abnormal keratinocyte growth and AD-like skin architecture.

- Inhibition of KLK5-mediated effects restored DSG1 expression and decreased AD-related cytokine expression, thus suggesting that KLK5 inhibition may be useful as a potential treatment for AD.

Capsule summary

Persistently increased serine protease kallikrein 5 modifies skin barrier proteins, upregulates AD-related cytokine expression and induces AD-like skin architecture. Inhibition of KLK5 may offer potential as a treatment strategy in AD.

Key word

Kallikrein 5, atopic dermatitis, skin barrier, serine protease inhibitor, SFTI

abbreviations

KLK5 (kallikrein), DSG1 (desmoglein 1), PAR2 (protease activated receptor 2), CAP18 (cathelicidin precursor cationic antimicrobial protein 18), AD (atopic dermatitis), NS (Netherton syndrome), FLG (filaggrin), UT (untransduced keratinocytes), AP (PAR2 agonist), TSLP (thymic stromal lymphopoietin), rKLK5 (recombinant KLK5).

Introduction

Tissue kallikreins (KLKs) are a family of fifteen (chymo)trypsin-like serine proteases which function through proteolytic cascades in the skin. Eight KLKs are expressed in the skin with KLK5 being one of the three most important, the others being KLK7 and KLK14[1]. KLK5 is produced as an inactive precursor from keratinocytes and activated by matriptase and KLK14[2,3], but can also undergo self-activation. It is able to activate other KLKs, therefore, KLK5 has been considered to be the initiator of KLK activation cascades within the skin[4].

KLK5 is expressed in the outmost layers of the epidermis, and the importance of its biological function in the epidermal barrier was initially discovered through studies on Netherton Syndrome (NS), a rare severe autosomal recessive skin disorder caused by mutations in the *SPINK5* gene[4,5]. In NS, *SPINK5* mutations cause loss of function of its encoded protein LEKTI, a multi-domain serine protease inhibitor, leading to elevated activity of KLK5. This results in cleavage of intercellular adhesion protein desmoglein 1 (DSG1), causing excessive desquamation of corneocytes and leading to a severely defective skin barrier, a major cause of early neonatal death in NS[6]. In addition to its involvement in DSG1 degradation, KLK5 is able to activate protease activated receptor 2 (PAR2), a subfamily of G protein-coupled receptors, and trigger expression of pro-inflammatory cytokines such as IL-8[7,8]. KLK5 is also involved in the innate immune system within the skin by cleaving the cathelicidin precursor cationic antimicrobial protein 18 (CAP18) at its c-terminus to produce 37 amino acid peptide LL-37, a major antimicrobial peptide with broad-spectrum antimicrobial activity[9].

Up-regulation of kallikreins including KLK5 has been reported in many chronic inflammatory skin diseases including atopic dermatitis (AD)[10,11]. AD is a multifactorial disease caused by complex interactions between genetic and environmental factors, with evidence that irritants (such as those contained in soaps) can further damage the skin barrier and exacerbate the inflammation in AD patients[12]. In the past decade, significant progress has been made in the area of molecular genetics with identification of several genes linked to AD including *SPINK5*, *KLK7* and *FLG*[13-15]. These

104 findings have led to the proposition that an impaired epidermal barrier is the primary event,

105 allowing percutaneous allergen penetration and causing an enhanced Th2-skewed immune-

106 response[16]. The induced inflammatory response further compromises barrier function, resulting in

107 abnormal expression, activity and assembly of skin barrier related proteins, enzymes and lipids.

108 Aberrant up-regulation of KLK5 in AD skin has been reported[10,11] and increased KLK5 may play a

109 key role in the pathogenesis of the dysfunctional skin. However, due to the complex interactions

110 between various cells in AD inflamed skin, it is difficult to dissect the exact role of up-regulated

111 KLK5 in AD skin.

112 In this study, we confirmed up-regulation of KLK5 and abnormal expression of KLK5 down-stream

113 molecules DSG1 and filaggrin (FLG), but not PAR2 in AD skin. We also identified significantly

114 increased KLK5 and PAR2 expressions in an *ex-vivo* dermatitis model, but not in the cell model

115 with persistent over-expression of KLK5, illustrating different responses of PAR2 to transient or

116 persistent KLK5 stimulation. We also demonstrated that increased IL-8, IL-10 and TSLP in

117 keratinocytes with persistently expressed KLK5 was independent of PAR2 activity, and that

118 inhibition of KLK5 activity with the serine protease inhibitor SFTI-G reduced cytokine production

119 and normalised DSG1 protein expression. Furthermore, persistent KLK5 over-expression alters

120 keratinocyte behaviour *in vivo*, resulting in epidermal acanthosis similar to that observed in AD skin,

121 indicating a key role for KLK5 in AD pathology.

122

123

124

125

126

127

128

Materials and Methods

<u>Skin biopsies and haematoxylin and eosin staining (H&E)</u>

Skin biopsies were taken from non-lesional and lesional skin from five AD patients. Five age-matched healthy donors were also obtained. This study was approved by the local ethics committee (LREC number 05/Q0508/106). Skin samples were formalin fixed paraffin embedded, and H&E staining was performed on 6 μm thickness paraffin skin sections using standard histochemistry techniques.

<u>Immunostaining and protein quantification</u>

Immunofluorescence and immunohistochemistry staining were carried out on frozen or paraffin embedded tissue sections using a purified anti-KLK5 mouse polyclonal antibody in 1:500 dilutions (Novus Biologicals, Abingdon, UK), or an anti-DSG1 mouse monoclonal antibody recognizing N-terminal extracellular domain (clone P124) in 1:100 dilutions (2B Scientific Ltd, Upper Heyford, UK), or an anti-FLG monoclonal antibody in 1:100 dilutions (Leica biosystems, Newcastle, UK), or an anti-involucrin mouse monoclonal antibody in 1:1000 (Sigma, Dorset, UK) or an anti-keratin 10 mouse monoclonal antibody (clone number LHP2, a gift from Royal London Hospital, UK). MolecularProbes secondary antibodies conjugated with florescence dye were obtained from Life Technologies (Paisley, UK). The detection of immunohistochemistry used biotinylated secondary antibodies and DAB substrate kit for peroxidase (Vector laboratories, Peterborough, UK). The staining procedures were as described by Di et al[17], and negative controls were performed in each staining with the secondary antibody alone.

The quantification of protein expression and activity in the epidermis was performed based on the staining intensity using software Image-Pro Plus v6.0 (Media Cybernetics, Cambridge, UK). Briefly images of three non-overlapped but adjacent regions in each section were recorded and saved digitally. The epidermis in each image was then highlighted as an area of interest (AOI) and the defined positive staining threshold was applied to the AOIs. The optical counts of positive staining

6

155   within AOIs were automatically counted based on the defined threshold and the expression or

156   activity in each AOI was calculated as mean staining intensity /area.

157

158   <u>Primary keratinocyte and keratinocyte cell line culture</u>

159   Primary keratinocytes and fibroblasts were isolated from skin biopsies by incubation with 0.25%

160   trypsin-EDTA (Life Technologies, Paisley, UK) 3 hours for keratinocytes and Serva 50 U/ml

161   collagenase NB6 (Universal Biologicals, Cambridge, UK) 2 hours for fibroblasts. Isolated primary

162   keratinocytes were then co-cultured with lethally irradiated 3T3 mouse fibroblasts and grown in

163   keratinocyte culture media. The media contained equal amount of DMEM and DMEM/Ham F12

164   (Life Technologies, Paisley, UK) supplemented with 10% FCS (Labtech, East Sussex, UK), 100

165   IU/ml of penicillin and 100 µg/ml of streptomycin (Life Technologies, Paisley, UK). Human

166   keratinocyte growth supplement was then added to the media at final concentrations of 10 ng/ml of

167   EGF (Bio-Rad AbD Serotec, Oxford, UK), 0.4 µg/ml of hydrocortisone, 5 µg/ml of transferrin, 5

168   µg/ml of insulin, $2x10^{-11}$ M of liothyronine and $1x10^{-10}$ M of cholera toxin (Sigma, Dorset, UK).

169   Ntert[18], a keratinocyte cell line was cultured in the same keratinocyte media. Fibroblasts were

170   cultured in DMEM supplemented with 10% FCS, 100 IU/ml of penicillin and 100 µg/ml of

171   streptomycin.

172

173   *Ex-vivo* dermatitis model and immunofluorescent staining

174   Skin from female breast tissue, obtained with informed consent and ethical approval (LREC

175   07/Q1704/59) following mastectomy was used as an *ex vivo* dermatitis model. The skin, which was

176   surplus to histopathology requirement, was placed in ice cold PBS immediately following removal

177   and stored on ice for a maximum of 2 hours, then placed into a 60 mm petri dish and the epidermal

178   surface carefully blotted dry. Rubber O-rings with a diameter of 8 mm were sealed on to the skin

179   using soft paraffin wax to create wells; care was taken to ensure that paraffin wax was applied only

180   to the area where the O-ring made contact with the skin in order to avoid altering the permeability

181 of the skin or the protease activity within the epidermis. To prevent the skin from drying out during

182 the incubation period, the remaining space within the petri dish was filled with DMEM, containing

183 10% FCS, at a depth of approximately 2 mm, ensuring no medium touched the epidermal surface of

184 the skin. Irritant substances and appropriate vehicle controls were applied carefully to separate

185 wells (50 µl solution each) and the skin incubated at 37°C with 5% CO_2 for the required length of

186 time. Following incubation, the entire irritant and vehicle control solutions were aspirated off the

187 epidermis and 6 mm punch biopsies were taken from the treated sites of the skin sample (without

188 removing the rubber O-rings) using sterile biopsy punches. A fresh biopsy punch was used for each

189 treatment to avoid cross-contamination, and the biopsy was removed from within the rubber O-ring

190 using forceps to ensure only treated skin was extracted. The biopsied tissue was placed in a 1.5 ml

191 eppendorf tube and snap frozen in liquid nitrogen. Samples were stored at -80$^\text{o}$C until further

192 investigations.

193 Following removal of skin biopsies from -80°C storage and embedding in Tissue-Tek® optimal

194 cutting temperature medium (OCT) (Sakura Finetek, Thatchem, UK), 8 µm tissue sections were cut

195 on a cryostat, allowed to dry onto poly-L-lysine coated glass slides, then fixed for 10 minutes in ice

196 cold acetone at -20°C. Slides were washed with TBS, blocked for 30 minutes with blocking buffer

197 followed by incubation with primary antibody in TBS overnight at 4°C. Slides were washed for 3 x

198 5 minutes in TBS, subsequently incubated with secondary antibody for 1 hour in the dark, then

199 washed in TBS for 3 x 5 minutes and, where necessary, counterstained by incubation with DAPI for

200 10 minutes, followed by a final wash of 3 x 5 minutes in TBS. Coverslips were attached using

201 Mowiol and the samples then visualised by fluorescence microscopy (Axioskop 2 MOT, Zeiss).

202 Slides were magnified at 100x and 400x and images digitally recorded (Axiocam, Zeiss). Slides

203 stained in the absence of primary antibody were used to set the exposure levels to reduce

204 background staining. Images were analysed using ImageJ v1.46 software, with 10 vertical regions

205 of interest (ROI's) from outer to inner surface of the epidermis selected from 1 field of view from 3

206 consecutive sections for each sample and the contribution from each layer along this measurement

207 was recorded. The 10 measured ROIs were normalised to 100% and the mean pixel intensity

208 obtained for every 5% of the depth (i.e. from outer to inner surface) of the epidermis. The minimum

209 average pixel intensity for a 5% section in the PBS sample was set at 1 and all other readings for the

210 sample set calculated relative to this value.

211

212 <u>Construction of lentiviral vectors and transduction of keratinocytes</u>

213 Human KLK5 cDNA was cloned into the pCCL lentiviral vector containing upstream spleen focus-

214 forming virus (SFFV) promoter and downstream enhanced green fluorescent protein (eGFP)

215 reporter gene linked to KLK5 via an internal ribosomal entry sequence from the endomyocarditis

216 virus. The vector encoding eGFP alone was used as negative control. Lentiviruses were produced

217 by co-transfecting 293T cells. Infectious lentiviruses were harvested 48 and 72 hours post-

218 transfection, and the culture supernatants were concentrated by ultracentrifugation. The lentivirus

219 concentration were titrated by viral copy number using qPCR and flow cytometry and the titres of

220 eGFP viral vector and KLK5/eGFP viral vector were 8×10^8 and 4×10^8 TU/ml, respectively.

221 Human primary keratinocytes and cell line Ntert were transduced by one round of exposure to

222 eGFP or KLK5/eGFP vectors at an MOI of 10. Transduced cells were subcultured for further

223 experiments.

224

225 <u>Intracellular calcium mobilization assay</u>

226 Measurement of intracellular calcium mobilization was performed using FluoForte Calcium Assay

227 kit (Enzo Life Sciences, Exeter, UK). Mobilization of intracellular calcium was detected utilizing a

228 fluorogenic calcium-binding dye. Keratinocytes were plated in 96-well plates at the density of $1 \times$

229 10^4 cells per well. After 24 hours, the growth medium was removed and 100µl of dye-loading

230 solution was added. The cells were further incubated with the dye-loading solution for 45 min at

231 37°C and then 15 minutes at room temperature. The cells were then inoculated with 100 µM of

232 PAR2 activating peptide SLIGKV-NH$_2$, (Bachem, Cambridge Bioscience, Cambridge, UK), and

9

233   intracellular calcium signal was recorded via real-time monitoring of fluorescence intensity at

234   excitation of 530 nm and emission of 570 nm using the microplate reader FLUOstar OPTIMA,

235   (BMG, Lutterworth, UK). Intracellular calcium mobilization was calculated as changes of

236   fluorescence intensity in relative fluorescence units (RFU) and the mobilisation curves were

237   generated by RFU values plotted against the time.

238

239   Western blotting

240   Cells were suspended in a cooled lysis buffer composed of 50 mM Tris-HCl pH 8.0, 150 mM NaCl,

241   5 mM EDTA, cocktail protease inhibitors and 1 mM PMSF. Samples were incubated for 15 minutes

242   at 4°C and then were centrifuged at 12,000 RPM for 15 minutes. The total protein concentration in

243   the supernatant of lysed sample was determined by Bio-Rad protein assay Kit (Bio-Rad,

244   Hertfordshire, UK). Samples were further diluted 5 times in 0.5 mM Tris-HCl pH 6.8 sample buffer

245   containing 100 mM DTT, 10% SDS, 30% glycerol, 0.001% bromphenol blue. Equal amounts of

246   total protein were loaded in SDS-PAGE. After electrophoresis, proteins were transferred to PVDF

247   membranes and incubated with primary antibody overnight. The following day, membranes were

248   incubated with secondary antibody conjugated with horseradish peroxidase (Sigma, Poole, UK),

249   and signals were detected using the ECL Prime system (GE Healthcare, Bucks, UK). Ponceau red

250   (Sigma-Aldrich, Poole, UK) staining was used as loading control for culture supernatants.

251

252   *In situ* zymography and casein gel zymography

253   I*n situ* zymography assay using casein-derived substrate measured the total protease activity in the

254   skin. Briefly, the frozen skin sections were rinsed with PBS containing 0.1% Triton X-100 (Sigma-

255   Aldrich, Poole, UK) and incubated at 37°C with 10 μg/ml casein conjugated with BODIPY TR-X

256   (Life Technologies, Paisley, UK) in the buffer containing 10 mM Tris-HCl, pH7.8 in a humid

257   chamber for two hours,. The fluorescent intensity was detected under a fluorescence microscope

258   and quantified using Image-Pro.

259 Casein gel zymography was used for cells that were cultured in keratinocyte culture media without

260 FCS for 48 hours. The culture media were then collected and concentrated using Amicon

261 centrifugal filter devices (Millipore, Watford, UK). Samples were re-dissolved in non-reducing

262 Novex® Tris-Glycine SDS sample buffer (Life Technologies, Paisley, UK) and separated on 12%

263 polyacrylamide gels copolymerized with casein substrate (Life Technologies, Paisley, UK). After

264 electrophoresis, the gels were soaked in renaturing buffer containing 50 mM Tris, pH 8 and 2.5%

265 Triton X-100 for 1 hour. The gels were then incubated in developing buffer containing 50 mM Tris,

266 pH 8 (Life Technologies, Paisley, UK) at 37°C overnight. Casein degrading activity was visualized

267 when the gels were stained with 1% Coomassie Brilliant blue (Sigma-Aldrich, Poole, UK).

268

269 <u>Human cytokine antibody array</u>

270 The cytokines in culture media collected from the different cell lines were assessed using The

271 Human Cytokine Antibody Array Panel A kit (R&D System, Oxfordshire, UK) according to the

272 manufactory's instruction. A total number of 36 cytokines were measured and the intensities of the

273 blots were quantified by densitometry. As each reference or target protein was blotted in duplicate,

274 mean pixel density from duplicate blots was calculated and normalised by reference blots.

275

276 <u>RT-PCR for IL-8</u>

277 Following RNA extraction using the RNeasy® Plus Mini Kit (Qiagen), a second genomic DNA

278 elimination step was employed to prevent genomic DNA contamination, and cDNA was then

279 synthesised using the RT^2 first strand kit (SABiocience). Quantitative PCR was performed in

280 duplicate wells for each time point using a 7900HT Fast Real-Time PCR System (Applied

281 Biosystems, CA, USA) and the data collected using SDS 2.4 software (Applied Biosystems, CA,

282 USA). The PCR protocol consisted of an initial cDNA denaturation at 95°C for 10 min, followed

283 by 35 cycles of denaturation at 95°C for 15 seconds and annealing and data collection at 60°C for

284 60 seconds. ΔCT values were calculated using the Ct value for the housekeeping gene 26S and

285 analysis of fold change in gene regulation was performed using automated Microsoft Excel analysis

286 tools from SABioscience.

287

288 <u>Enzyme linked immunosorbent assay (ELISA)</u>

289 Cells were seeded in 24 well plates and cultured until confluence, then cultured in serum free media

290 for 48 hours before culture media were collected and concentrated using Amicon centrifugal filter

291 devices (Millipore, Watford, UK). The total protein concentration was quantified using Bio-Rad

292 protein assay kit. The level of IL-8 was measured using IL-8 ELISA kit (BD Biosciences, Oxford,

293 UK). TSLP and IL-10 were quantified using ELISA kits from eBioscience (eBioscience, Hatfield,

294 UK). All sample reads were normalized to the total protein concentration.

295

296 <u>Bio-engineered skin sheet and grafting onto immunodeficient mice</u>

297 The methods of generating bio-engineered skin sheet and grafting to mice were as described by Di

298 et al[19]. Briefly, primary human keratinocytes were seeded on the top of a fibrin matrix populated

299 with primary human fibroblasts. After keratinocytes reached confluence, the bioengineered skin

300 constructs were grafted onto the dorsum of 6 weeks old female immunodeficient mice (NMRI

301 strain, Charles River, UK). 8 weeks after grafting, skin samples from grafts were taken post-mortem

302 and formalin fixed and paraffin-embedded or OCT-embedded. H&E staining and immunostaining

303 for KLK5, FLG and DSG1, and zymographics were performed on these tissues.

304

305

306

307

308

309

Results

Increased expression and activity of KLK5 in AD skin

Skin biopsies taken from lesional and non-lesional skin in five children with AD were examined for epidermal morphology and KLK5 expression. Five age-matched normal donor skin biopsies were used as controls. Compared to normal skin, AD lesional skin exhibited epidermal changes including acanthosis, spongiosis, parakeratosis and elongated rete ridges. Non-lesional skin also showed histopathological characteristics consistent with the disease, but far less prominent than those observed in lesional skin (**Figure 1A. a-c**). The expression of KLK5, as detected by immunostaining, was localised in the cornified layer in normal skin, whereas in AD skin, especially in the lesional skin, KLK5 was present in the granular layer and upper stratum spinosum with high staining intensity (**Figure 1A. d-f and Supplementary materials, Figure S1**). Quantification of KLK5 based on mean optical staining intensity/area further demonstrated significant increased expression of KLK5 in both lesional and non-lesional AD skin, compared to the normal skin ($p<0.05$) (**Figure 1B**). As DSG1 is the proteolytic substrate of KLK5, and FLG can be degraded by elastase 2 which is a serine protease activated by KLK5 in the skin[20], DSG1 and FLG expressions were also examined by immunostaining. Both FLG and DSG1 expression were significantly reduced in lesional skin of AD ($p<0.05$) (**Figure 1A. g-i & j-l, Figure 1B**). The protease activity in the skin were further examined by *in situ* staining, and results showed a similar location and staining pattern to KLK5 expression with more diffuse and enhanced fluoresecence intensity in the AD skin (**Figure 1A. m-o, Figure 1B and Supplementary materials, Figure S2**). Although the caseinolytic serine protease assay detects total protease activity, as KLK5 is a major serine protease in the skin[2] and the protease activity closely matched the extent and distribution of KLK5 protein expression, it is likely that KLK5 is a significant contributor to the increased activity of serine protease observed in the AD skin.

335 **Transient up-regulation of KLK5 stimulated PAR2, but persistant activated KLK5**

336 **desensitised PAR2**

337 The expression of the KLK5 targeted molecule PAR2 was further examined in the donor skin (n=5)

338 and AD non-lesional and lesional skin by immunostaining. No significant changes in PAR2

339 expression was noted in lesional, non-lesional AD skin and normal donor skin (p>0.05) (**Figure 1A.**

340 **p-r, Figure 1B**), although there was a fluctuation of PAR2 expression level among individuals.

341 This result suggests that up-regulated KLK5 does not modify PAR2 in AD skin. Considering that

342 the up-regulation of KLK5 was likely to be chronic and persistant in AD skin, we speculated that

343 the response of PAR2 to KLK5 might differ between AD skin and skin with transient KLK5 up-

344 regulation. To determine this, the influence of transiently increased KLK5 on PAR2 was tested

345 using an *ex-vivo* irritant dermatological model in which irritants were applied onto normal skin

346 cultured *in vitro*. Following the application of croton oil or SDS or acetone for 30 minutes on the

347 *ex-vivo* skin model, increased epidermal expression of KLK5 and PAR2 were detected in the

348 epidermis (**Figure 2. a**). Quantification using image analysis confirmed significantly higher

349 expression of both KLK5 and PAR2 across all layers of the epidermis **(Figure 2. b-e)**.

350 The effect of persistently increased KLK5 on PAR2 was tested in the keratinocyte cell line Ntert

351 (KLK5-Ntert) or primary keratinocytes (KLK5-pKC) ectopically over-expressing KLK5. Cells

352 transduced with eGFP vector alone were used as control (GFP-Ntert or GFP-pKC). The

353 transduction efficiency in both KLK5 transduced cells and GFP transduced cells was nearly 60% as

354 determined by eGFP expression. Overexpression of KLK5 in KLK5-transduced cells and culture

355 media was confirmed by western blotting (**Figure 3. a&c**). The activity of KLK5 was further

356 assessed by zymography. Active KLK5 was detected in the culture media collected from KLK5

357 transduced cell culture (**Figure 3. d**), but not in cell lysates (**Figure3. b**). KLK5 is synthesized as

358 inactive pre-pro-KLK5 (precursor or zymogene) which is then translocated into the endoplasmic

359 reticulum in cells (see review by Debela M *et al*)[21]. Following the removal of the signal peptide

360 (~30 amino acids), the pre-pro-KLK5 becomes pro-KLK5 that is secreted into the extracellular

361 space and subsequently becomes activated upon release of its 37 amino acids propeptide from the

362 N-terminus of KLK5. Thus, the KLK5 extracted from the cells would not contain the final activated

363 KLK5 and it is not surprising that there was no positive digested band detected in zymography

364 loaded with cell lysates. In contrast, a digested band was seen in zympgraphy loaded with culture

365 medium from cells over expressing KLK5/eGFP as a result of the culture medium containing the

366 active form of KLK5. Although a ~70kDa band was present on both western blotting and

367 zymography, the intensity of the protein band remained unchanged among cell lysates from

368 untransduced cells, cells transduced with GFP alone and KLK5/GFP, therefore this was considered

369 to represent a nonspecific protein, but having a proteolytic activity on casein-derived substrate.

370 The durability of KLK5 expression in both KLK5-Ntert and KLK5-pKC was assessed following

371 propagation of transduced cells and there was no decline in KLK5 expression over this time as

372 determined by eGFP expression, indicating persistent KLK5 expression in the KLK5-cell model

373 (**Supplementary materials, Figure S3**). As a previous study showed that PAR2 was mainly

374 expressed in differentiated keratinocytes, the Ntert cell line was checked for differentiation markers

375 keratin 10 and involucrin and results showed positive expression for both proteins (**Supplementary**

376 **materials, Figure S4**). The activity of PAR2 and a KLK5 down-stream target was then examined

377 in untransfected Ntert (UT-Ntert), GFP-Ntert and KLK5-Ntert by a PAR2-dependent calcium

378 mobilisation assay. Mobilisation of calcium was observed in the untransfected keratinocytes after

379 addition of a PAR2 agonist (AP), and similarly following addition of recombinant KLK5 (rKLK5),

380 albeit slightly later than that induced by AP (**Figure 4. a**), confirming that KLK5 was able to

381 activate PAR2. In contrast, a decline in calcium mobilisation was detected in KLK5-Ntert cells

382 compared to that in GFP-Ntert (**Figure 4. b**). Thus, a different PAR2 dependent calcium

383 mobilisation response was observed in cells with persistent expression of KLK5 versus cells with

384 transient rKLK5 stimulation.

385 PAR2, like many other receptors, can be desensitized if continuously or repeatedly exposed to its

386 agonist[22,23], and these results suggest that persistent over-expression of KLK5 could desensitise the

387 PAR2 receptor resulting in a lower response of PAR2 to its agonist AP. Since PAR2 desensitisation

388 can be reversed by removal of PAR2 activators, we looked at calcium mobilisation when KLK5-

389 Ntert cells were treated with the serine protease inhibitor SFTI-G, an analogue derived from the

390 naturally occurring substance sunflower trypsin inhibitor 1[24]. Following treatment with 100μM

391 SFTI-G overnight, the PAR2 dependent calcium mobilisation in KLK5-Ntert cells recovered to

392 levels similar to that in GFP-Ntert and untransfected keratinocytes (**Figure 4. c**).

393

394 **Persistently activated KLK5 induced cytokine expression/secretion despite PAR2**

395 **desensitisation**

396 Activated PAR2 induced pro-inflammatory cytokine elevation and secretion, including of IL-8, has

397 been reported[25]. In the *ex-vivo* irritant dermatological skin model, increased IL-8 mRNA expression

398 was detected by RT-PCR within 12 hours following exposure to SDS and to a lesser extent at 12

399 hours following application of croton oil (**Figure 5. a**). In the KLK5-pKC cells with persistent

400 KLK5 expression, IL-8 protein, measured by cytokine antibody array, was also increased (**Figure**

401 **5.b&c**). In addition, IL-10 was elevated in KLK5-pKC cells (**Figure 5. b&c**), but other cytokines

402 including IL-1, IL-4, IL-6 and IFN-gamma were not (**Supplementary materials, Table S1**). TSLP,

403 a prominent pro-inflammatory cytokine in AD skin also showed increased expression in KLK5-

404 pKC cells as measured by ELISA (**Figure 5. c**). However, increased IL-10 and TSLP were not

405 detected in cells transiently challenged with rKLK5 (data not shown).

406

407 **Inhibition of persistent KLK5 activity reversed KLK5 effects on DSG1 and cytokine**

408 **production**

409 To examine the downstream effects of inhibition of persistently raised KLK5 activity, primary

410 keratinocytes transduced with KLK5 (KLK5-pKC) or eGFP (GFP-pKC) were cultured in serum

411 free media inoculated with 100 μM of serine protease inhibitor SFTI-G for twenty-four hours.

412 Although the level of secreted KLK5 in culture media, as determined by western blot, remained

16

413 elevated in the KLK5-pKC cells 24 hours post SFTI-G treatment, the expression of full length

414 DSG1 was restored in treated KLK5-cells compared to untreated cells, whereas there was no

415 significant change in the level of DSG1 in GFP-pKC cells before (-) and after SFTI-G (+)

416 treatment, indicating the suppression of KLK5 activity by SFTI-G in the KLK-5 culture (**Figure 6.**

417 **a**). It was noticed that in KLK5-pKC cells, there was no DSG1 detected. The DSG1 antibody used

418 in the study was a monoclonal antibody (clone P124) recognizing the N-terminal extracellular

419 domain of DSG1 and full length DSG1. Primary keratinocytes were used for untreated as well as

420 treated experiments, and treated cells showed a DSG1 band. Therefore, no DSG1 band in KLK5-

421 pKC cells without SFTI-G treatment was most likely due to DSG1 levels being to too low to be

422 detected and/or the antibody does not recognize the cytoplasm domain of DSG1 alone following the

423 cleavage of the extracellular domain by over-expressed/activated KLK5. Cytokines IL-8, IL-10 and

424 TSLP were also significantly reduced in SFTI-G treated KLK5-pKC cells, compared to untreated

425 KLK5-pKC cells, and these changes were not observed in treated or untreated GFP-cells as

426 confirmed by both cytokine antibody array and ELISA (**Figure 5.b, 6.b&c**, **Supplementary**

427 **materials, Table S1**).

428

429 **Keratinocytes with persistent activated KLK5 exhibit an AD-like epidermal architecture**

430 To examine the influence of persistently up-regulated KLK5 activity on epidermal architecture *in*

431 *vivo*, primary keratinocytes from the non-lesional skin in a patient with AD (AD-pKC), or primary

432 normal keratinocytes ectopically over-expressing KLK5 (KLK5-pKC) or GFP (GFP-pKC) were

433 cultured *in vitro* as bio-engineered skin and grafted onto immuno-deficient mice. 8 weeks post-

434 grafting, the skin from the grafted area was harvested. Grafts generated from KLK5-pKCs and AD-

435 pKC showed AD-like morphology, with acanthosis, mild parakeratosis and enlarged intercellular

436 spaces compared to the GFP-pKC graft (**Figure 7. a-c**). Increased expression of KLK5 and protease

437 activity and decreased DSG1 were observed in both KLK5-pKC and AD-pKC grafts compared to

438 GFP-cell graft (**Figure 7. d-l**), which were analogous to findings in AD skin. Altered FLG

17

439   expression was also detected in KLK5-pKC and AD-pKC grafts, it was more evident in the upper

440   stratum spinosum similar to that seen in the AD skin (**Figure 7. m-o and Figure 1A. h&i).** As the

441   FLG antibody used for the study only detects FLG produced from human cells, the mouse-human

442   skin boundary was easily visible in the FLG stained skin, indicating that the keratinocytes within

443   the grafts were of human origin (**Figure 7. g-i**). In addition, the mouse-human skin boundary

444   images showed an increased thickness of mouse epidermis (acanthosis) next to the grafts generated

445   by KLK5-pKC and AD-pKC, but not by the GFP-pKC, which may have resulted from a paracrine

446   effect of activated KLK5 secreted from these grafts.

447

448

449

450

451

452

453

454

455

456

457

458

459

460

461

462

Discussion

Up regulated KLK5 together with skin barrier defects in AD has been reported in previous studies[10,11,26], which have shown that both genetic and environmental factors can cause aberrant KLK5 activity. Indeed, as AD shares a number of clinical features with NS, it has been speculated that AD might also share some pathological mechanisms of dysfunctional skin barrier with NS[27,28]. Genome-wide association studies have shown several single nucleotide polymorphisms (SNPs) in *SPINK5* associated with AD, in particular Glu420Lys[28] and functional investigations have further confirmed that Glu420Lys SNP alters SPINK5 encoded protein LEKTI proteolytic activation and results in dysregulation of proteases including the KLKs[29]. Environmental factors that disrupt the skin barrier, including irritants and infection, and trigger KLK5 up-regulation have also been reported[30]. In this study, we have demonstrated that the irritants croton oil and SDS increase KLK5 and PAR2 expression, but that transient KLK5 expression seems to have different effects on PAR2 expression/activity than that observed with persistent KLK5 expression.

KLK5 activation of PAR2 has been demonstrated previously[31] and we also showed rKLK5 activated PAR2 in this study using an intracellular calcium mobilization fluorescence assay. The fluorescence peak induced by rKLK5 was, however, delayed 40-50 seconds compared to the peak induced by the PAR2 agonist (AP). This difference in peak time was likely to be due to the tethered ligand mechanism with regards maximum rate of PAR2 activation by KLK5. Oikonomopoulou and colleagues[31] have reported that KLK5 activation of PAR2 is a two-step process involving cleavage and tethered ligand binding to the PAR2 receptor, whereas a one-step process is involved in the PAR2 agonist directly binding to the receptor.

The signalling pathway of KLK5-PAR2-NFκB-cytokines has been recognised for more than a decade[32,33], but most studies have been carried out in models with transient exposure to exogenous rKLK5[31]. PAR2 can exhibit desensitization due to continuous or repeated stimulation by its agonist, leading to reduced responsiveness[34]. AD is a chronic skin condition, and up-regulated KLK5 activity in affected skin is most likely to be persistent than transient. However, the examination of

489 PAR2 activity in skin *in situ* is technically difficult. Currently, the activity of PAR2 is assessed by

490 intra-cellular calcium mobilization in live cells following stimulation/inhibition with its

491 agonist/antagonist. Tissues from AD skin or murine AD models are generally fixed/embedded or

492 snap frozen, and thus are not suitable for use in the calcium mobilization assay. There is an indirect

493 way to check PAR2 activity by examination of PAR receptor internalization, e.g. by tracking GFP-

494 tagged PAR2 fusion protein trafficking[35] or by analysing the distribution of activated (cytoplasmic)

495 and unactivated (cell membrane) PAR2 receptor[36], but these also require cell-culture models rather

496 than skin tissue. However, although the desensitisation of PAR2 in the skin *in situ* cannot be

497 measured directly, previous work by Moniaga and colleagues[37] supports our view that PAR2 is

498 desensitised in AD-like skin lesions. In their study[37], a PAR2 agonist could up-regulate TLSP in

499 murine keratinocytes following transient (one-off) stimulation, but only a marginal increase of

500 TSLP production was noted in the skin of flaky tail mice following repeated topical application of

501 dust mite for 7 weeks; this discrepancy of TLSP production between transient stimulation in cell

502 culture and repeated challenge in mouse skin was probably because the repeated challenge caused

503 PAR2 desensitisation, resulting in low PAR2 activity. Related to this, an *in vivo* study by Briot and

504 colleagues showed that TLSP production was independent of PAR2 activation and that PAR2 was

505 not central to the production of the skin inflammation when there was persistent KLK5 activity[38].

506 In mice with double knockout of SPINK5-/- and PAR2-/- and high KLK activity, the deletion of

507 PAR2 in the adult double knockout-grafted skin did not result in the reduction of TLSP and did not

508 suppress the skin inflammation[38]. This result suggests that the inflammatory skin in Netherton

509 syndrome and AD is not solely caused by PAR2 activation.

510 Based on our observations in the AD skin with persistent KLK5 overexpression and the *ex-vivo*

511 irritant dermatological skin model mimicking a transiently increased KLK, we demonstrated that

512 PAR2 had a higher response to transient KLK5 stimulation, but had a weak response to persistent

513 KLK5 stimulation. Interestingly, despite the low activity of PAR2 in cells overexpressing KLK5,

514 these cells up-regulated and secreted pro-inflammatory and Th2-polarizing cytokines, including IL-

20

515   8, IL-10 and TSLP, indicating that persistent KLK5 induced IL-8, IL-10 and TSLP. The exact

516   pathway of persistent KLK5 expression/activity induced IL8, IL10 and TLSP secretion in KLK5-

517   pKC remains unclear, and further investigations will be required to elucidate this. The keratinocyte-

518   based nature of our KLK5 over-expressing model, which lacks immune cells, meant that it was not

519   possible to investigate cytokine secretion from immune cells following KLK5 activation, which

520   may explain why our cytokine antibody array data did not show elevation of other

521   cytokines/chemokines reported in AD patients (such as IL-6, IL-4, GM-CSF, IL-1 and TNFα).

522   The influence of activated KLK5 on epidermal architecture in the *in vivo* human:murine chimeric

523   skin graft model, which showed AD-like skin architecture in grafts generated using cells over-

524   expressing KLK5, further indicated that KLK5 plays a key role in this process. Similar observations

525   have also been detected using a transgenic mouse model over-expressing KLK5[39]. Furthermore, as

526   the human:murine chimeric skin graft model was immunodeficient and maintained in specific

527   pathogen-free environment, our results suggest that the AD-like histopathological features and

528   abnormal barrier protein expression in the epidermis generated by AD-cells and KLK5-pKC cells

529   were a specific consequence of persistent up-regulation of KLK5 in the keratinocytes.

530   Our study also suggests that increased KLK5 in AD skin should not simply be viewed as a

531   'biomarker' in this skin disorder, but as a protease which has significant functional impact in this

532   condition. In AD patients, environmental factors can trigger the cytokine cascade and stimulate a

533   Th2-skewed inflammatory infiltrate through the initial defective skin barrier, resulting in

534   susceptibility to allergy or 'atopy' ("outside-inside" aetiological mechanism)[16,40]. The induced

535   inflammatory response further compromises barrier function, causing keratinocyte damage and

536   inducing upregulation of certain molecules, such as KLK5. The initial damage secondary to

537   increased KLK5 forms a vicious cycle of inflammation-induced barrier impairment in AD (outside-

538   inside-outside)[16].

539   Amongst the currently known inhibitors of kallikreins[41-43], the naturally occurring cyclic peptide

540   SFTI has been extensively investigated due to it being amenable to chemical manipulation which

541 has allowed for the creation of synthetic variants[44-46]. We used the analogue SFTI-G derived from

542 SFTI[24] to control KLK5 activity and our *in vitro* results showed a normalised DSG1 expression,

543 depletion of depressed PAR2 dependent calcium mobilisation and reduction of IL-8, IL-10 and

544 TSLP. Thus, reducing KLK5 activity could offer a therapeutic option for the treatment of AD,

545 where control of higher KLK5 activity might help to reverse (at least part of) the AD phenotype in

546 patients with this disorder.

547

Acknowledgements

References

1. Lundwall A and Brattsand M, Kallikrein-related peptidases, *Cell Mol Life Sci,* 2008 Jul, 65(13):2019-2038.

2. Brattsand M et al., A proteolytic cascade of kallikreins in the stratum corneum, *J Invest Dermatol,* 2005 Jan, 124(1):198-203.

3. Sales KU et al., Matriptase initiates activation of epidermal pro-kallikrein and disease onset in a mouse model of Netherton syndrome, *Nat Genet,* 2010 Aug, 42(8):676-683.

4. Caubet C et al., Degradation of corneodesmosome proteins by two serine proteases of the kallikrein family, SCTE/KLK5/hK5 and SCCE/KLK7/hK7, *J Invest Dermatol,* 2004 May, 122(5):1235-1244.

5. Chavanas S et al., Mutations in SPINK5, encoding a serine protease inhibitor, cause Netherton syndrome, *Nat Genet,* 2000 Jun, 25(2):141-142.

6. Descargues P et al., Corneodesmosomal cadherins are preferential targets of stratum corneum trypsin- and chymotrypsin-like hyperactivity in Netherton syndrome, *J Invest Dermatol,* 2006 Jul, 126(7):1622-1632.

7. Stefansson K et al., Kallikrein-related peptidase 14 may be a major contributor to trypsin-like proteolytic activity in human stratum corneum, *Biol Chem,* 2006 Jun, 387(6):761-768.

8. Steinhoff M et al., Proteinase-activated receptors: transducers of proteinase-mediated signaling in inflammation and immune response, *Endocr Rev,* 2005 Feb, 26(1):1-43.

9. Yamasaki K et al., Kallikrein-mediated proteolysis regulates the antimicrobial effects of cathelicidins in skin, *FASEB J,* 2006 Oct, 20(12):2068-2080.

10. Komatsu N et al., Human tissue kallikrein expression in the stratum corneum and serum of atopic dermatitis patients, *Exp Dermatol,* 2007 Jun, 16(6):513-519.

11. Voegeli R et al., Increased stratum corneum serine protease activity in acute eczematous atopic skin, *Br J Dermatol,* 2009 Jul, 161(1):70-77.

12. Angelova-Fischer I, Irritants and Skin Barrier Function, *Curr Probl Dermatol,* 2016, 49:80-89.

13. Palmer CN et al., Common loss-of-function variants of the epidermal barrier protein filaggrin are a major predisposing factor for atopic dermatitis, *Nat Genet,* 2006 Apr, 38(4):441-446.

14. Vasilopoulos Y et al., Genetic association between an AACC insertion in the 3'UTR of the stratum corneum chymotryptic enzyme gene and atopic dermatitis, *J Invest Dermatol,* 2004 Jul, 123(1):62-66.

15. Walley AJ et al., Linkage and allelic association of chromosome 5 cytokine cluster genetic markers with atopy and asthma associated traits, *Genomics,* 2001 Feb, 72(1):15-20.

16. Elias PM and Schmuth M, Abnormal skin barrier in the etiopathogenesis of atopic dermatitis, *Curr Allergy Asthma Rep,* 2009 Jul, 9(4):265-272.

17. Di WL et al., Human Involucrin Promoter Mediates Repression-Resistant and Compartment-Specific LEKTI Expression, *Hum Gene Ther,* 2012 Jan, 23(1):83-90.

18. Dickson MA et al., Human keratinocytes that express hTERT and also bypass a p16(INK4a)-enforced mechanism that limits life span become immortal yet retain normal growth and differentiation characteristics, *Mol Cell Biol,* 2000 Feb, 20(4):1436-1447.

19. Di WL et al., Ex-vivo gene therapy restores LEKTI activity and corrects the architecture of Netherton syndrome-derived skin grafts, *Mol Ther,* 2011 Feb, 19(2):408-416.

20. Bonnart C et al., Elastase 2 is expressed in human and mouse epidermis and impairs skin barrier function in Netherton syndrome through filaggrin and lipid misprocessing, *J Clin Invest,* 2010 Mar, 120(3):871-882.

21. Debela M et al., Structures and specificity of the human kallikrein-related peptidases KLK 4, 5, 6, and 7, *Biol Chem,* 2008 Jun, 389(6):623-632.

22. Bohm SK et al., Mechanisms of desensitization and resensitization of proteinase-activated receptor-2, *J Biol Chem,* 1996 Sep, 271(36):22003-22016.

23. Stefansson K et al., Activation of proteinase-activated receptor-2 by human kallikrein-related peptidases, *J Invest Dermatol,* 2008 Jan, 128(1):18-25.

24. Shariff L et al., Sunflower trypsin inhibitor (SFTI-1) analogues of synthetic and biological origin via N-S acyl transfer:potential inhibitors of human Kallikrein-5 (KLK5), *Tetrahedron,* 2014, 70:7675-7680.

25. Hou L et al., Immunolocalization of protease-activated receptor-2 in skin: receptor activation stimulates interleukin-8 secretion by keratinocytes in vitro, *Immunology,* 1998 Jul, 94(3):356-362.

26. Komatsu N et al., Multiple tissue kallikrein mRNA and protein expression in normal skin and skin diseases, *Br J Dermatol,* 2005 Aug, 153(2):274-281.

27. Di WL et al., A heterozygous null mutation combined with the G1258A polymorphism of SPINK5 causes impaired LEKTI function and abnormal expression of skin barrier proteins, *Br J Dermatol,* 2009 Aug, 161(2):404-412.

28. Walley AJ et al., Gene polymorphism in Netherton and common atopic disease, *Nat Genet,* 2001 Oct, 29(2):175-178.

29. Fortugno P et al., The 420K LEKTI variant alters LEKTI proteolytic activation and results in protease deregulation: implications for atopic dermatitis, *Hum Mol Genet,* 2012 Oct, 21(19):4187-4200.

30. Torma H, Lindberg M, and Berne B, Skin barrier disruption by sodium lauryl sulfate-exposure alters the expressions of involucrin, transglutaminase 1, profilaggrin, and kallikreins during the repair phase in human skin in vivo, *J Invest Dermatol,* 2008 May, 128(5):1212-1219.

31. Oikonomopoulou K et al., Kallikrein-mediated cell signalling: targeting proteinase-activated receptors (PARs), *Biol Chem,* 2006 Jun, 387(6):817-824.

32. Rallabhandi P et al., Analysis of proteinase-activated receptor 2 and TLR4 signal transduction: a novel paradigm for receptor cooperativity, *J Biol Chem,* 2008 Sep, 283(36):24314-24325.

33. Buddenkotte J et al., Agonists of proteinase-activated receptor-2 stimulate upregulation of intercellular cell adhesion molecule-1 in primary human keratinocytes via activation of NF-kappa B, *J Invest Dermatol,* 2005 Jan, 124(1):38-45.

34. Soh UJ et al., Signal transduction by protease-activated receptors, *Br J Pharmacol,* 2010 May, 160(2):191-203.

35. Ramsay AJ et al., Kallikrein-related peptidase 4 (KLK4) initiates intracellular signaling via protease-activated receptors (PARs). KLK4 and PAR-2 are co-expressed during prostate cancer progression, *J Biol Chem,* 2008 May, 283(18):12293-12304.

36. Gratio V et al., Kallikrein-related peptidase 14 acts on proteinase-activated receptor 2 to induce signaling pathway in colon cancer cells, *Am J Pathol,* 2011 Nov, 179(5):2625-2636.

37. Moniaga CS et al., Protease activity enhances production of thymic stromal lymphopoietin and basophil accumulation in flaky tail mice, *Am J Pathol,* 2013 Mar, 182(3):841-851.

38. Briot A et al., Par2 inactivation inhibits early production of TSLP, but not cutaneous inflammation, in Netherton syndrome adult mouse model, *J Invest Dermatol,* 2010 Dec, 130(12):2736-2742.

39. Furio L et al., Transgenic kallikrein 5 mice reproduce major cutaneous and systemic hallmarks of Netherton syndrome, *J Exp Med,* 2014 Mar, 211(3):499-513.

40. Cork MJ et al., Epidermal barrier dysfunction in atopic dermatitis, *J Invest Dermatol,* 2009 Aug, 129(8):1892-1908.

41. Tan X et al., Toward the first class of suicide inhibitors of kallikreins involved in skin diseases, *J Med Chem,* 2015 Jan, 58(2):598-612.

42. Tan X et al., 1,2,4-Triazole derivatives as transient inactivators of kallikreins involved in skin diseases, *Bioorg Med Chem Lett,* 2013 Aug, 23(16):4547-4551.

43. Teixeira TS et al., Biological evaluation and docking studies of natural isocoumarins as inhibitors for human kallikrein 5 and 7, *Bioorg Med Chem Lett,* 2011 Oct, 21(20):6112-6115.

44. de Veer SJ et al., Mechanism-based selection of a potent kallikrein-related peptidase 7 inhibitor from a versatile library based on the sunflower trypsin inhibitor SFTI-1, *Biopolymers,* 2013 Sep, 100(5):510-518.

45. Swedberg JE et al., Substrate-guided design of a potent and selective kallikrein-related peptidase inhibitor for kallikrein 4, *Chem Biol,* 2009 Jun, 16(6):633-643.

46. de Veer SJ et al., Engineered protease inhibitors based on sunflower trypsin inhibitor-1 (SFTI-1) provide insights into the role of sequence and conformation in Laskowski mechanism inhibition, *Biochem J,* 2015 Jul, 469(2):243-253.

Legends

Figure 1.   Skin morphology and protein expression in AD

A: Skin sections from normal donor (n=5) and AD skin (n=5) were examined by H&E (a-c), immunostaining (d-l & p-r), and *in situ* zymography (m-o). Green/brown colour represents protein expression or protease activity. Nuclei were stained in blue colour. Scale bar = 50 μm.

 B: Quantification of staining intensity (n=3 per sample) was measured by mean staining intensity/area using ImagePro.

Figure 2. **Increased KLK5 and PAR2 expression in *ex-vivo* dermatitis skin model**

Immunofluorescence staining of epidermal KLK5 and PAR2 following application of 3% croton oil and 5% SDS compared with acetone-treated and PBS-treated skin. Quantification of relative KLK5 (b,d) and PAR2 (c,e) expression from stratum corneum to basal layer (0%-100% depth respectively). KLK5 (n=9, n=7), PAR2 (n=7, n=6) for 3% croton oil and 5% SDS respectively.

Figure 3.   Characterisation of keratinocyte over expressing KLK5

The expression and activity of KLK5 in cell lysate (a,b) and culture media (c,d) from the cells transfected with KLK5 gene were examined by Western blot (left panel) and gel zymography (right panel). β-actin were used as loading controls. UT = untransduced cells; eGFP = cells transduced with eGFP alone vector; KLK5 = cells transduced with KLK5/eGFP vector and rKLK = activated recombinant KLK5 protein (where rKLK was added directly to the gel as a positive zymography control).

Figure 4. PAR2-dependent calcium mobilisation in keratinocytes

PAR2-dependent calcium mobilisation was measured in untransfected Ntert cells challenged with AP or rKLK5 (a); cells transfected with GFP or KLK5 challenged with AP (b); and cells transfected with GFP or KLK5, treated with SFTI-G and then challenged with AP (c). PBS was used as negative control.

Figure 5. Cytokine expression in keratinocytes

Cytokine levels were measured in the *ex-vivo* skin model with transiently up-regulated KLK5 using RT-PCR for IL8 (a); KLK5-pKC cells with persistent KLK5 expression using antibody array blots (b). The IL-8 and IL-10 levels detected by cytokine antibody array and quantified by mean pixel density, and TSLP level measured by ELISA are shown in the bar chart (c). Data in (a) are shown relative to PBS-treated skin.

Figure 6. The inhibition of KLK5 by serine protease inhibitor SFTI-G

Primary keratinocytes transduced with GFP or KLK5 gene were treated with 100μM of SFTI-G overnight. KLK5 in culture media and DSG1 in cell lysates were measured by Western blot (a). Cytokine secretions in the culture media following SFTI-G treatment were measured by cytockine antibody array (b) and confirmed by ELISA (c). The symbol * is representative of statistical significance (p<0.05) and NS stands for non-significance.

Figure 7. Persistent KLK5 activity induced AD-like skin changes

A: Skin graft sections from human:murine skin graft mice were examined for morphology by H&E (a-c), KLK5 (d-f) expression by immunohistochemistry, DSG1 (j-l) and FLG (m-o) expression by immunofluorescence, and protease activity (g-i) by *in situ* zymography. Brown

and green colour show protein expression/protease activity and purple and blue colour show stained nuclei. Scale Bar= 50 μm.
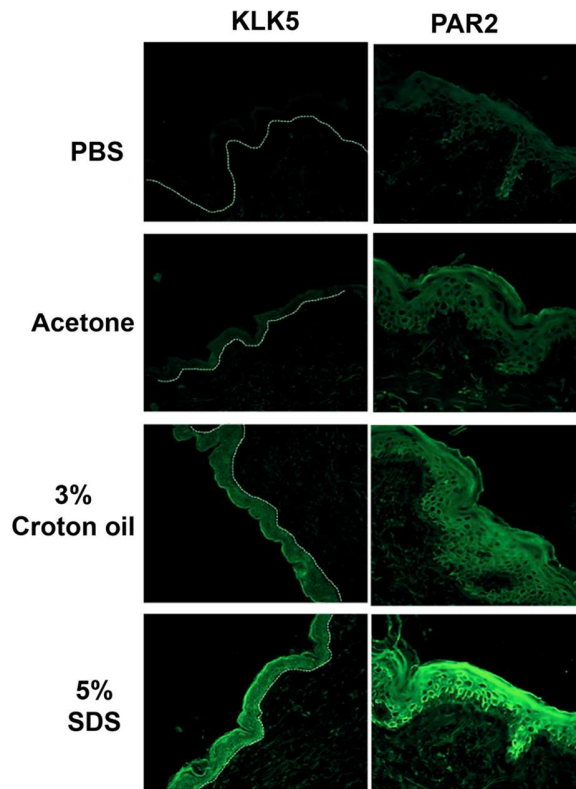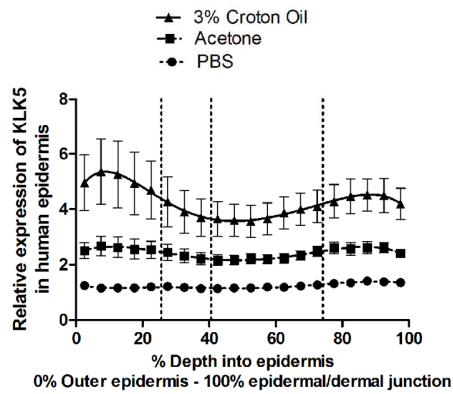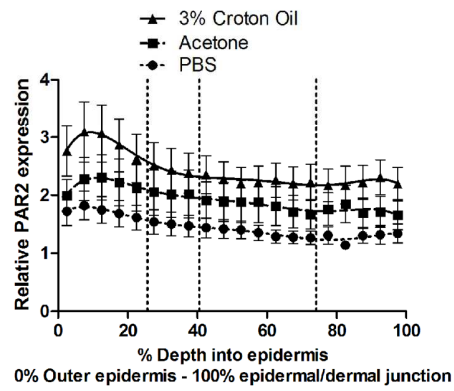
Cell lysates

a

UT eGFP KLK5 kDa

b

UT eGFP KLK5

— 76 —

— 52 —

← KLK5

— 38 —

— 17 —

β-Actin 42kDa

Culture media

c

UT eGFP KLK5 rKLK5 kDa

d

UT eGFP KLK5 rKLK5

— 52 —

— 38 —

← KLK5

— 17 —

a

b

c

a

b

c

a

b

After SFTI-G treatment

GFP-pKC   KLK5-pKC

c

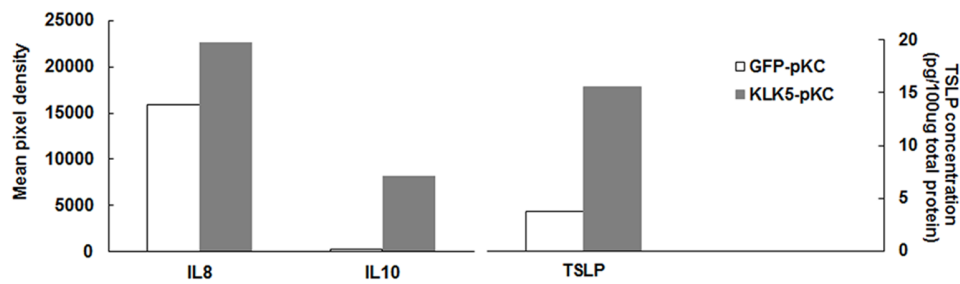**Normal skin**   **AD non-lesion**   **AD lesion**

control1/
patient1

control2/
patient2

control3/
patient3

control4/
patient4

control5/
patient5

	Normal skin	**AD non-lesion**	**AD lesion**

control1/
patient 1

control2/
patient2

control3/
patient3
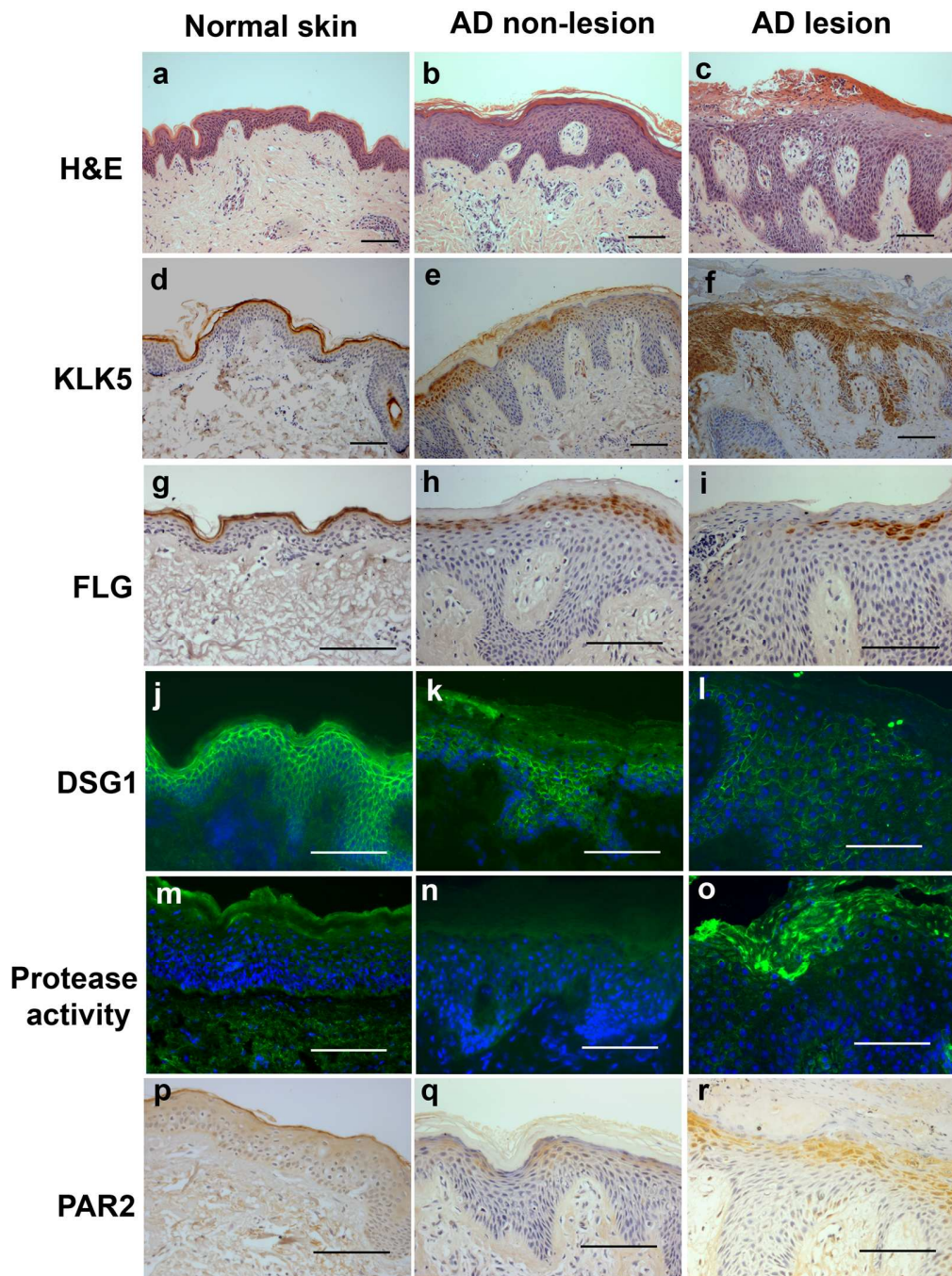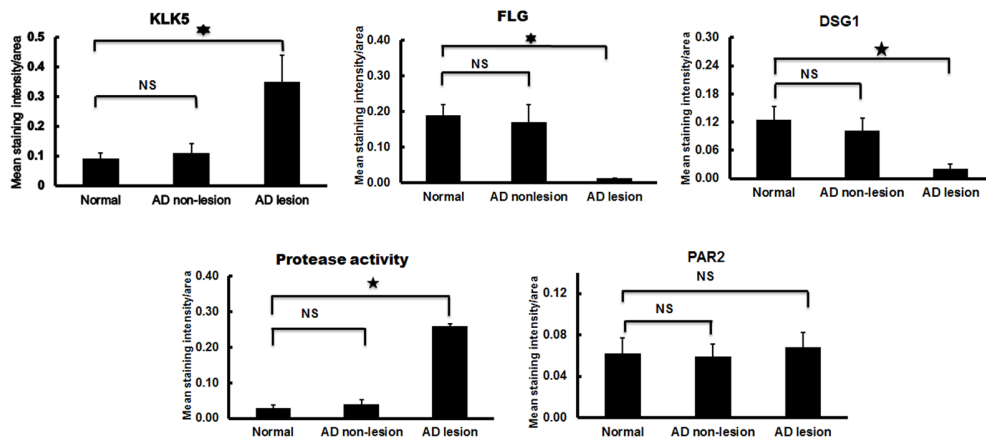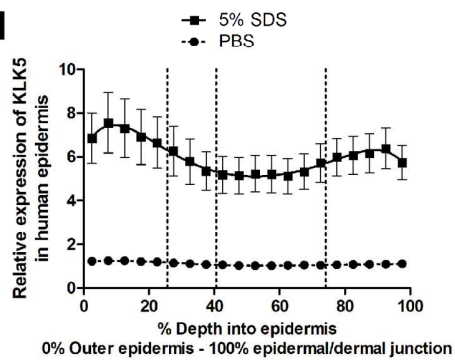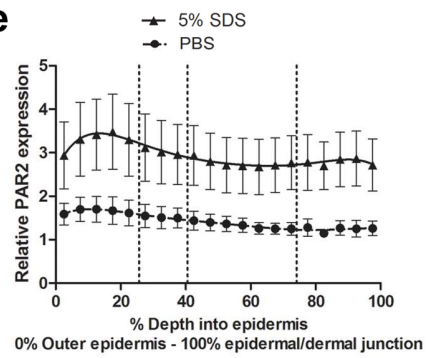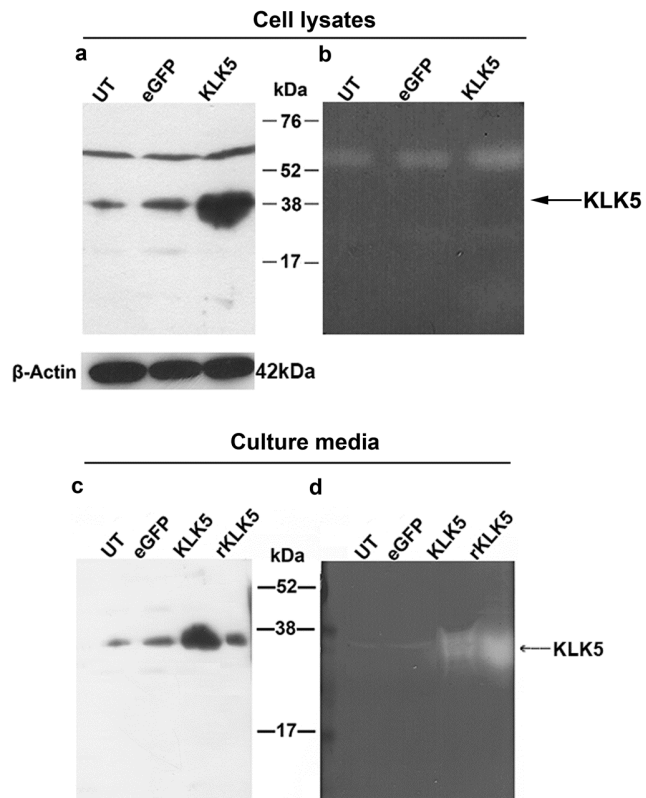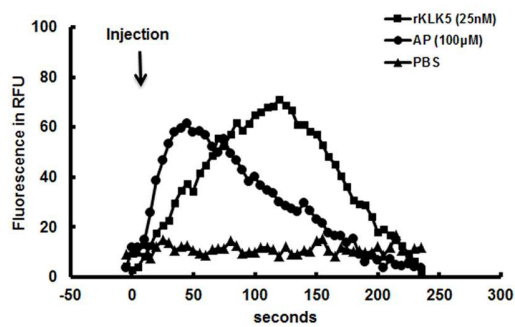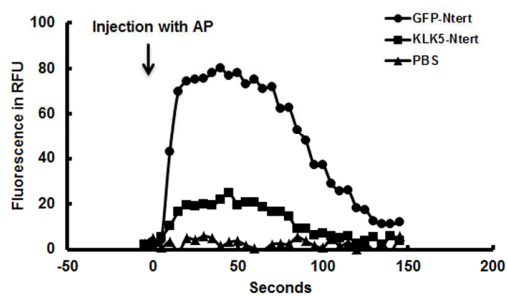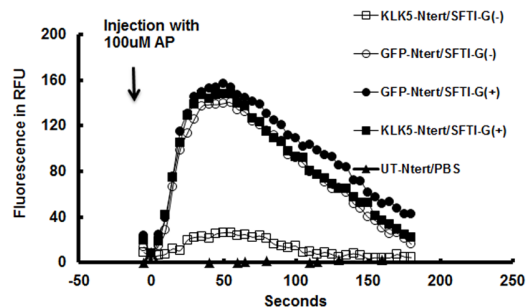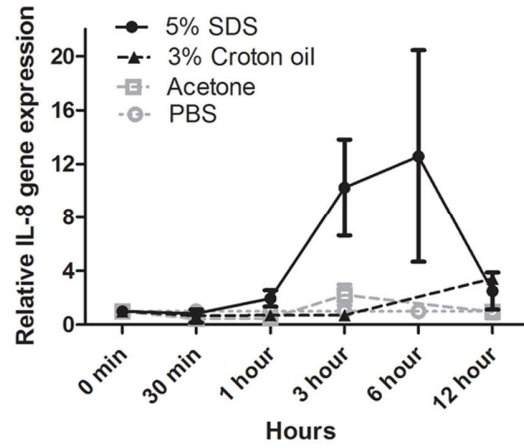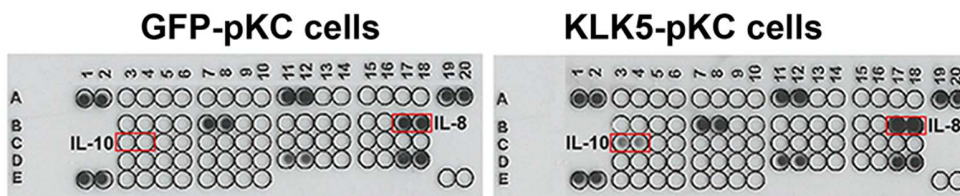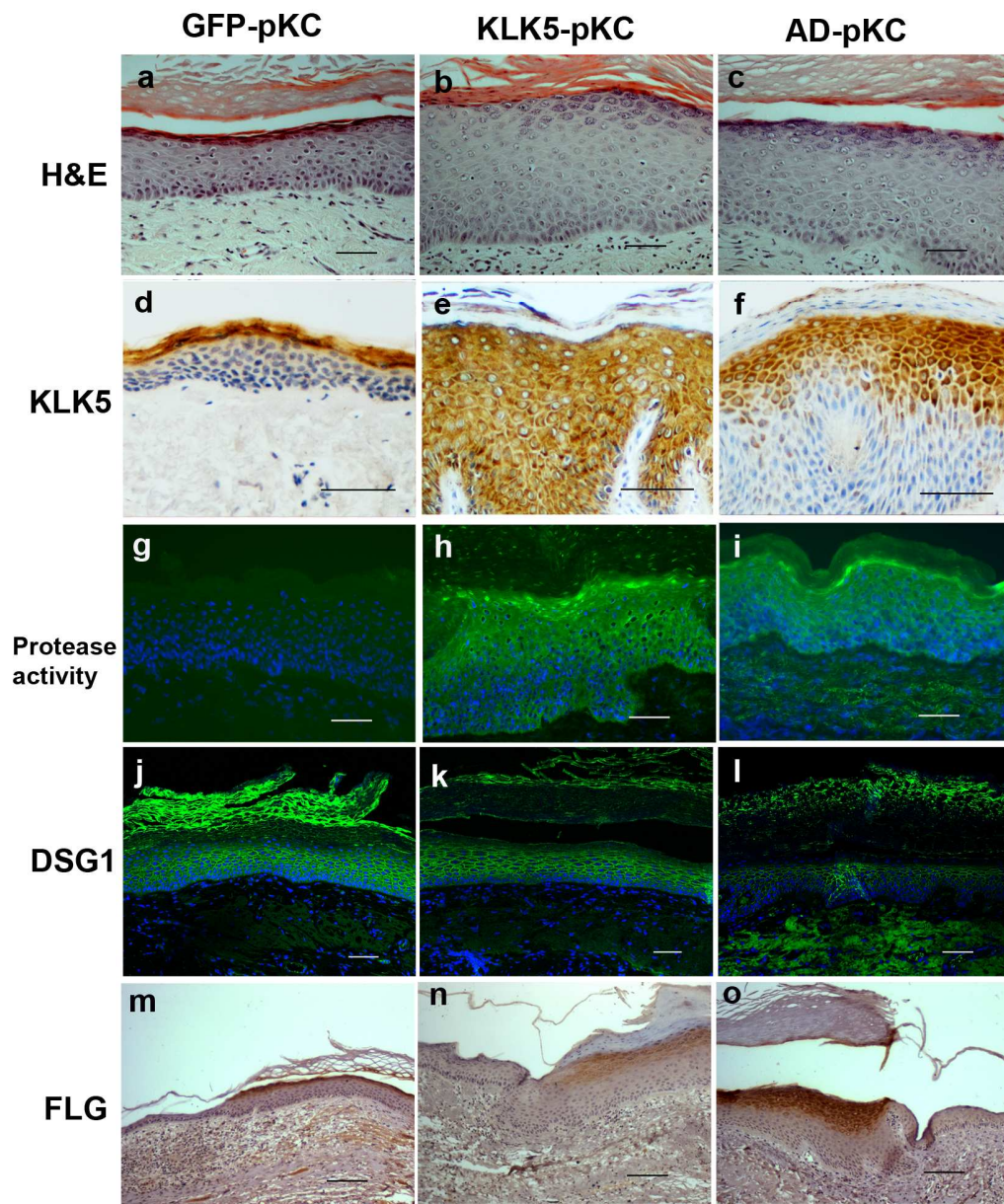
control4/
patient4

Supplementary materials
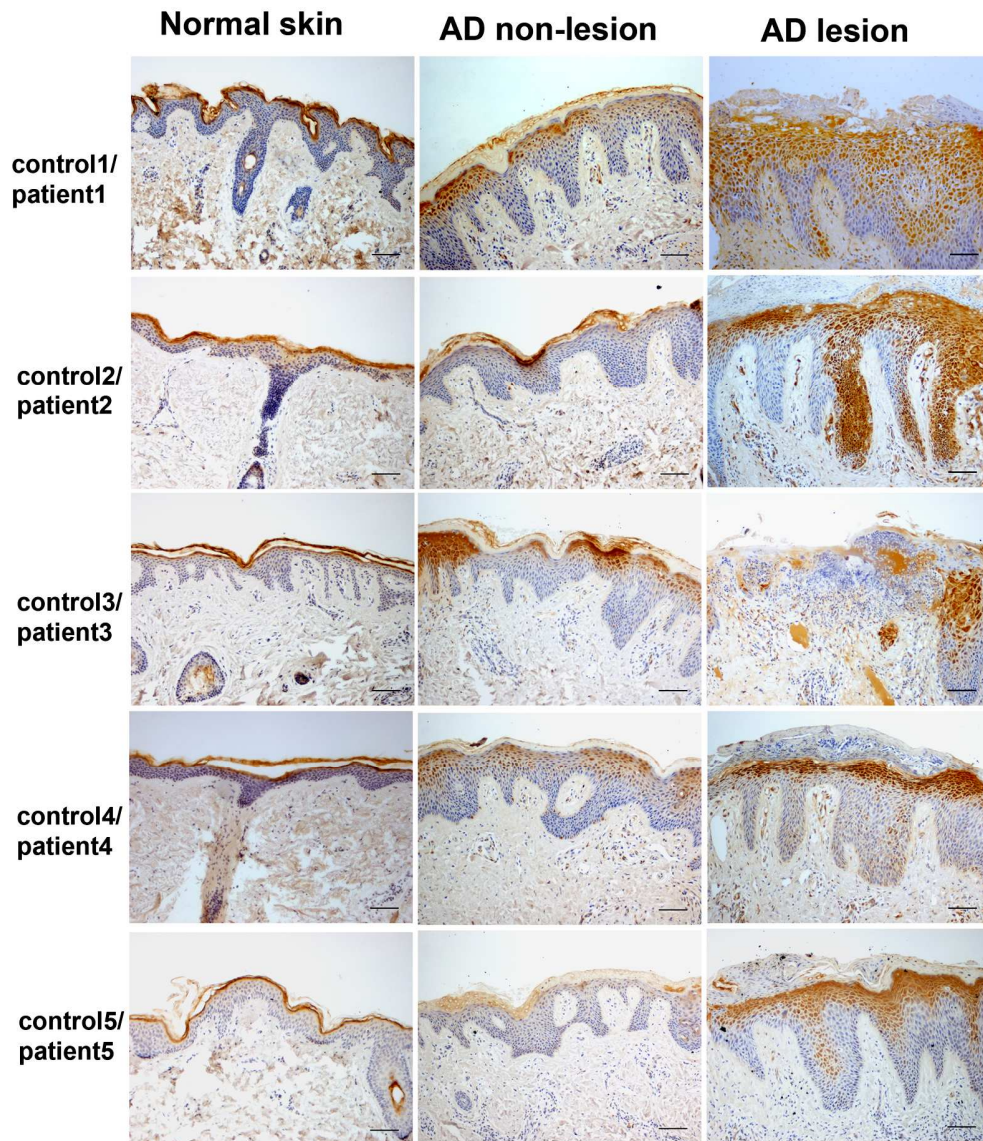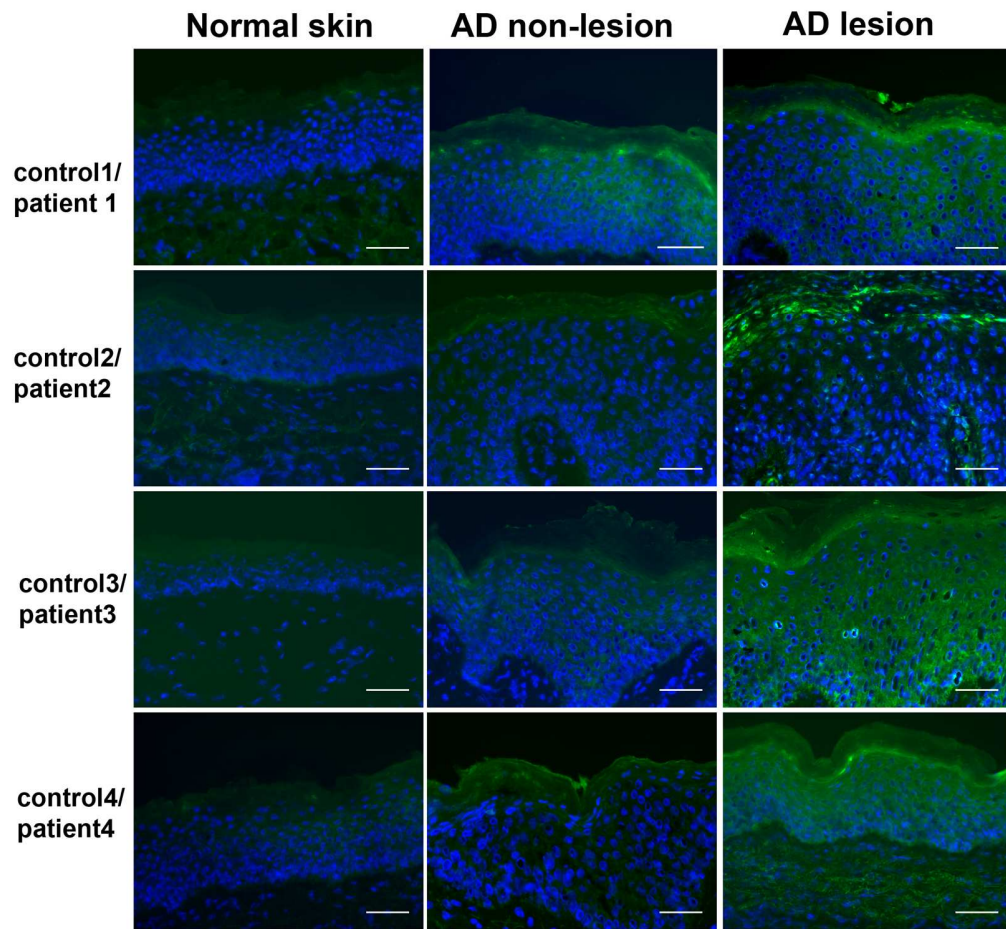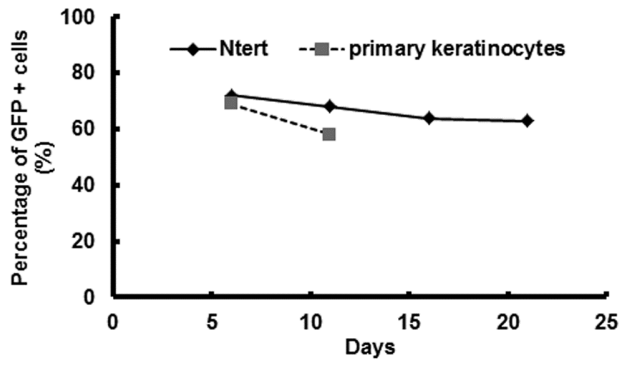
Table S1. Quantification of dots by densitometry for cytokine antibody array

Coordinate of the plate	Target/control	Mean pixel density			
		GFP-pKC		KLK5-pKC	
		SFTI (-)	SFTI (+)	SFTI (-)	SFTI (+)
A1,A2	Reference spot	17896	17221	17701	17193
A3,A4	C5/C5a	232	294	245	302
A5,A6	CD40 ligand	216	259	241	226
A7,A8	G-CSF	308	299	327	302
A9,A10	GM-CSF	341	367	319	298
A11,A12	GRO-alpha	18958	19020	19110	19212
A13,A14	I-309	327	381	338	306
A15,A16	sICAM-1	404	394	420	441
A17,A18	IFN-gamma	336	385	312	397
A19,A20	Reference spot	16350	16361	16222	16119
B3,B4	IL-1a	188	226	209	198
B5,B6	IL-1b	217	275	232	202
B7,B8	IL-1ra	15933	15659	15899	16021
B9,B10	IL-2	297	310	268	289
B11,B12	IL-4	322	338	301	297
B13,B14	IL-5	275	311	291	298
B15,B16	IL-6	397	344	380	393
B17,B18	IL-8	15922	15273	22598	16276
C3,C4	IL-10	224	243	8236	268
C5,C6	IL-12 p70	313	289	326	301

C7,C8	IL-13	406	484	415	461
C9,C10	IL-16	359	331	360	314
C11,C12	IL-17	448	429	465	438
C13,C14	IL-17E	385	375	397	408
C15,C16	IL-23	535	521	519	569
C17,C18	IL-27	449	425	456	406
D3,D4	IL-32a	398	331	386	350
D5,D6	IP-10	421	452	409	398
D7,D8	ITAC	415	429	406	466
D9,D10	MCP-1	399	411	394	429
D11,D12	MIF	12868	12525	13310	12806
D13,D14	MIP-1a	275	310	298	322
D15,D16	MIP-1b	393	404	415	438
D17,D18	Serpin E1	18256	18010	18166	18125
E1,E2	Reference spot	17510	17725	17566	17621
E3,E4	RANTES	435	509	466	428
E5,E6	SDF-1	449	399	425	462
E7,E8	TNF-alpha	398	439	412	402
E9,E10	sTERM-1	421	461	435	489
E19,E20	Negative control	275	211	261	293

Legends

Figure S1. KLK5 expression in non-lesional and lesional skin from five AD patients

Skin sections from normal donor (n=5, control 1-5, left panel) and AD patients (n=5, patient 1-5) from non-lesional (middle panel) and lesional (right panel) skin were examined for KLK5 expression using immunohistochemistry. Brown colour represents protein expression and blue colour shows nuclei stain. Scale bar = 100 μm.

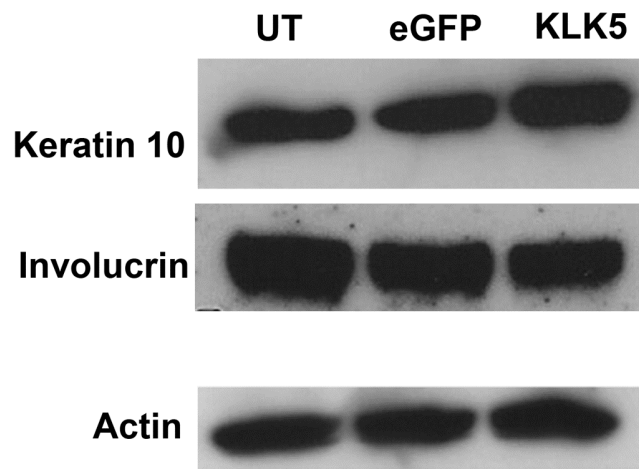**Figure S2. *In situ* protease activity in non-lesional and lesional skin from AD patients**

Skin sections from normal donor (n=4, control 1-4, left panel) and AD patients (n=4, patient 1-4) from non-lesional (middle panel) and lesional (right panel) skin were examined for total protease activity by *in situ* zymography. Green colour represents protease activity, whereas nuclei are stained blue. Scale bar = 50 μm.

Figure S3. Stability of transgene KLK5 expression in keratinocytes

Primary keratinocytes and Ntert keratinocyte cell line were transduced with KLK5/eGFP transgene and the stability of transgene in cells was assessed by GFP positive cells (GFP+) using flow cytometry. Primary keratinocytes were only monitored for a period of 12 days due to proliferative lifespan of primary cells in *in vitro* culture.

Figure S4. Differentiation markers in Ntert keratinocytes

Keratin 10 and involucrin expression in cell lysates from untransduced Ntert keratinocytes (UT), or transduced with KLK5 (KLK5) or eGFP vector alone (eGFP) were assayed by Western blot. Positive expressions of both proteins indicated a proportion of differentiated cells in the Ntert cell line.

UT   eGFP   KLK5

Keratin 10

Involucrin

Actin